HYDROLOGICAL PROCESSES, VOL. 5, 81-100 (1991)

ON THE EXTRACTION OF CHANNEL NETWORKS FROM DIGITAL ELEVATION DATA

DAVID G. TARBOTON,* RAFAEL L. BRAS, AND IGNACIO RODRIGUEZ-ITURBE†
Ralph M. Parsons Laboratory, Department of Civil Engineering, Massachusetts Institute of Technology, Cambridge, MA, U.S.A.

ABSTRACT

Channel networks with artibtrary drainage density or resolution can be extracted from digital elevation data. However, for digital elevation data derived networks to be useful they have to be extracted at the correct length scale or drainage density. Here we suggest a criterion for determining the appropriate drainage density at which to extract networks from digital elevation data. The criterion is basically to extract the highest resolution (highest drainage density) network that satisfies scaling laws that have traditionally been found to hold for channel networks. Procedures that use this criterion are presented and tested on 21 digital elevation data sets well distributed throughout the U.S.

KEY WORDS Drainage density Digital Elevation Models Fluvial geomorphology River basins Mapping Cartography

INTRODUCTION

The advent of digital elevation models (DEMs) has resulted in the evolution of procedures to automatically map or derive channel networks from DEMs. This has obvious applications in cartography, geographic information systems, hydrologic modelling, and geomorphology where analysis and use of channel networks can now be achieved using computers instead of tediously digitizing or measuring from topographic maps. Some procedures using DEMs allow for the extraction of networks with arbitrary drainage density, i.e. resolution of networks to an arbitrary scale. Care needs to be exercised to ensure that networks are extracted from DEMs at an appropriate scale. This scale should correspond to the networks obtained by more traditional methods, such as from high resolution topographic maps or field work. However the drawing of blue lines on maps usually involves some subjective judgement by the cartographer.

Here methods for extracting networks from DEMs that produce networks that have properties consistent with those traditionally attributed to channel networks are suggested. In particular, we will extract the highest resolution channel network consistent with these traditional properties. In the next section we first review some of the properties attributed to channel networks and then review procedures for extracting networks from DEMs. Following this we propose two complementary procedures to rationally select the scale at which to extract channel networks. We then describe each of these procedures in detail and give results that compare the drainage density obtained from these procedures and other procedures in the literature.

REVIEW

The quantitative description of river networks was pioneered by workers such as Horton (1932, 1945), Strahler (1952, 1957), and Shreve (1966). The terminology we use summarized below is due to them. A river network is idealized as a trivalent planted tree, the root of which is the *outlet* or point farthest downstream. *Sources* are points farthest upstream, and a point at which two upstream channels join to form one

*Now at Utah Water Research Laboratory, Utah State University.
†At the Iowa Institute of Hydraulic Research, University of Iowa.

0885-6087/91/010081-20$10.00

Received and accepted 6 September 1990

downstream channel is called a *junction* or *node*. *Exterior links* are the segments of channel between a source and the first junction downstream and *interior links* are the segments of channel between two successive nodes or a node and the outlet. Each link has certain properties: *length* along the stream; *height*, the elevation difference between upstream and downstream nodes; average *slope*, height divided by length; *contributing area*, the total area draining through the link measured at the downstream end, and *local area*, the area draining directly into a link, i.e. not through any other links.

Ordering systems are used to group or categorize links or segments of channels. A major contribution of Horton (1932, 1945) was the introduction of a downstream ordering system. Strahler (1952, 1957) revised Horton's scheme to avoid some ambiguities. The revised Horton/Strahler ordering system is as follows. All exterior links have order 1. When two upstream links of the same order joint the downstream link has order increased by 1. When two upstream links of different order join the downstream link takes the higher order or the two incoming upstream links. Strahler streams are segments of channel consisting of links of the same order.

Horton/Strahler ordering is usually used in characterizing a river network according to the Horton ratios. The ratio of number of streams, length of streams, area of streams, and slope of streams between successive orders is approximately constant. A semilog plot of the number, length, area, and slope of streams against order plots as a straight line. The ratio or 'Horton number' is obtained from the slope of the straight line fit to such plots, the procedure being called a 'Horton analysis'. Mathematically the ratios are

$$R_b = N_{w-1}/N_w,\ R_l = L_w/L_{w-1},\ R_a = A_w/A_{w-1},\ R_s = S_{w-1}/S_w. \tag{1}$$

where N_w is the number of streams of order w, L_w is the mean length of streams of order w, A_w is the mean area contributing to streams of order w, and S_w is the mean slope of streams of order w. R_b, R_l, R_a, and R_s are bifurcation, length, area, and slope ratios, respectively. Since the ratios are approximately constant, the above geometric descriptors are called 'Horton's laws'. The area law above was not explicitly stated by Horton, and is due to Schumm (1956).

Leopold and Miller (1956) extended Horton's ideas by showing that the log of many hydraulic variables are approximate linear functions of basin order. This behaviour is due to the fact that most quantities depend strongly on the size of the drainage basin. A common measure of size or scale is basin area and the dependence of a general variable on area is often expressed by a power law

$$X \propto A^b \tag{2}$$

with b a constant. This implies

$$\log X \propto \log A \tag{3}$$

and since order is proportional to log A (area law) the linear relationships with order follow.

Horton/Strahler stream order is a topological, dimensionless measure of size or scale of a channel segment or network. A physical scale associated with the dissection of the landscape by a river network is drainage density, defined by Horton (1932, 1945) as

$$D_d = \frac{L_T}{A} \tag{4}$$

where L_T is the total length of streams and A is contributing area.

It is widely recognized that elevation, related to potential energy, is an important part of the network and we need to understand the structure and scaling of river networks with the third dimension, elevation, included. Qualitatively, streams are steep near their sources and flatter downstream. This is quantified by Horton's slope law which implies an exponential decrease of slope with order.

$$S_w = (R_s S_1) R_s^{-w} = R_s S_1 e^{-w \ln R_s} \tag{5}$$

Broscoe (1959) noted that the average drop H_w along Strahler streams of order w was approximately constant, i.e. independent of order. This 'constant drop law' is sometimes added to Horton's laws and Yang (1971) claims that it is due to a variational principle, equal distribution of stream power. Recognize that on average $H_w = S_w L_w$, so H_w constant implies

$$\frac{S_{w-1}}{S_w} = \frac{L_w}{L_{w-1}} \tag{6}$$

i.e., $R_s = R_l$. Typically R_s is close to R_l but it is not evident whether this coincidence is responsible for the constant drop law or is due to the constant drop law.

Flint (1974), building on the power law relationships of Wolman (1955), Leopold and Maddock (1953), Leopold and Miller (1956), and Leopold, *et al.* (1964) finds slope empirically related to contributing area by

$$S = CA^{-\theta} \tag{7}$$

with θ ranging from 0·37 to 0·83 with a mean of 0·6. Substituting in Horton's area and slope laws Flint (1974) gets

$$\theta = \frac{\ln R_s}{\ln R_a} \tag{8}$$

again showing the connections between power law scaling with area and exponential scaling with order (Horton's slope law).

Gupta and Waymire (1989) point out the close connection between power law scaling and notions of statistical self-similarity and suggest that link slopes may be statistically self-similar. However Tarboton *et al.* (1989) show that the second moment properties of channel slopes do not support this simple self similarity, but a more general multiscaling.

There has over the last decade been a growing interest in the use of digital elevation data in geomorphology and hydrology, specifically including the analysis of channel networks. This has resulted in the development of procedures for processing digital elevation data and extracting channel networks. O'Callaghan and Mark (1984) provide a good review of the early development in this field, as well as suggesting the algorithms on which much of this work is based.

O'Callaghan and Mark (1984) define a digital elevation model (DEM) as any numeric or digital representation of the elevations of all or part of a planetary surface. They restrict themselves to the most commonly used data structure for DEMs: the regular square grid. In such a grid elevations are available as a matrix of points equally spaced in two orthogonal directions. Other data structures have been used for DEMs in hydrological analysis. O'Callaghan and Mark (1984) suggest that triangular irregular networks (TIN) which include channels directly as triangle edges may have substantial advantages. Palacios-Velez and Cuevas-Renaud (1986) develop procedures using TIN networks. Contour based DEMs have been used with some success by O'Loughlin (1986) and Moore, *et al.* (1988). These have the advantage of dividing the catchment into natural units related to water flow, i.e. polygons formed by equipotential lines and their orthogonals, streamlines but are more demanding computationally, requiring at least an order of magnitude more points in contour line form than in regular grid form to adequately describe an elevation surface (Moore *et al.*, 1988). Carrara (1988) discusses schemes for interpolation of a grid-based DEM from contour data. These schemes range from general (moving average, splines, etc.) to morphology dependent algorithms that endeavour to interpolate the way a skilful reader would interpolate contour maps.

We used grid-based DEM data structures because the majority of United States Geological Survey (U.S.G.S.) DEM data sets are grid-based and grid-based procedures are simple and unambiguous. Many of

the important concepts in grid based DEM work are defined by O'Callaghan and Mark (1984), Mark (1988), and Jenson and Domingue (1988). Elevations are stored in an *elevation matrix* arranged in a grid with each entry giving the elevation of a point. The location within the matrix implies the spatial location of the point, so only elevation values need to be stored (as opposed to TIN networks that have to store x and y location and elevation data for each point and contour-based structures that store strings of x and y locations along a contour).

At this point it is useful to define some terminology appearing in the analysis of DEMs. A *pit* is defined as a point or set of adjacent points surrounded by neighbours that have higher elevations. A *drainage direction matrix* contains a set of pointers from each grid cell or pixel to one of its neighbours. Usually pointers are in the direction of steepest slope. The drainage direction matrix defines a drainage direction network as a forest of rooted subtrees. A *drainage accumulation function* is defined as an operator which given the drainage direction matrix and a weight matrix determines an *accumulated area matrix* such that each element in the area matrix represents the sum of the weight of all elements in the matrix which drain to that element. If the weights are all set at one, then the area matrix gives the total contributing area in number of elements or pixels.

O'Callaghan and Mark (1984) suggest defining channels on a DEM as all points with accumulated area above some threshold. Mark (1988) notes that at horizontal scales of 10 m or greater true pits or closed depressions are rare in natural earth topography, being restricted to a few special geomorphic environments (e.g. glaciated or karst). Pits occur frequently in DEMs due to data errors and sampling effects (e.g. a narrow channel may pass between grid points). Mark (1988) suggests pit removal based on actual drainage patterns (in the form of digitized stream channels) or by a local 'flooding' procedure where pits are made to drain towards the point at which water would overflow from the pit. Jenson and Domingue (1988) describe an algorithm that does this.

The procedure for identifying channels suggested by O'Callaghan and Mark (1984) and Mark (1988) is basically:

1. Pit removal and calculation of drainage direction matrix.
2. Calculation of the accumulated area matrix.
3. Define channels as pixels exceeding an accumulated area threshold.

This is the procedure used here. We focus on obtaining a physically justifiable accumulation area threshold.

Band (1986), following Peuker and Douglas (1975) has suggested the use of local operators to flag upward concave pixels as potential stream points. The Peuker and Douglas (1975) algorithm flags the pixel of highest elevation from each possible square of four adjacent pixels. After one sweep of the matrix the unmarked pixels represent drainage courses. The set of points obtained is not necessarily connected so Band (1986) describes several thinning and connection procedures. This approach has the advantage that no arbitrarily chosen support area has to be specified, however, there is no physical basis for it and to work properly it requires smoothing of the data. Below we will compare drainage density estimated from the Peuker and Douglas algorithm with that from the procedures we are suggesting.

DATA

Table I gives a list of all the digital elevation model data sets used in this work and their exact location, identified by their outlet pixel. Figure 1 shows their location in the United States. Table II gives statistics of the adjustments to the elevation data required to fill in pits for some typical data sets. We believe that the effect of these adjustments is relatively minor and in any case the pit filling procedure is the only automatic pit removal option we know of.

A RATIONAL CRITERIA FOR SELECTION OF SUPPORT AREA

In extracting channel networks from digital elevation models it is important that the networks extracted be close to what traditional workers using maps or fieldwork would regard as channel networks. The question

Table I. Digital elevation model data sets

Acroym	Name	Map quadrangles used	Outlet location Easting/ longitude	Outlet location Northing/ latitude	Pixel size
W7	Subbasin no. 7 in Walnut Gulch Experimental watershed	Hay Mtn. (AZ)	585360m	3511140m	30m
W15	Subbasin no. 15 in Walnut Gulch Experimental watershed	Hay Mtn., Tombstone (AZ)	590940m	3509040m	30m
W15A2S	Subbasin no. 15 in Walnut Gulch Experimental watershed	Hay Mtn., Tombstone (AZ)	590895m	3508965m	60m
CALD	Big Creek	Calder NW, NE, SW and SE (ID)	567330m	5235300m	30m
SPOKBC	Big Creek	Spokane E (ID)	116°06'39"	47°16'18"	3"(62·6 × 92·67m)
NELK	North Fork Cour d'Alene river	Spokane E (ID)	116°14'27"	47°35'51"	3"(62·6 × 92·67m)
STJOE	St. Joe River	Spokane E, Hamilton W, Wallace W (ID)	116°16'15"	47°18'36"	3"(62·6 × 92·67m)
STJOEUP	St. Joe River	Simmons Peak SE and SW, Pole Mtn., Bacon Peak, Chamberlain Mtn., Illinois Peak SE and SW (ID,MO)	623040m	5217360m	30m
STREGIS	St. Regis River	Wallace NE, Slatese NW, NE and SE, Haughan NE, NW, SE and SW, Simmons Peak NE, Illinois Peak NW (MO)	611670m	5239860m	30m
STREGISDMA	St. Regis River	Wallace W (MO)	115°08'06"	47°17'51"	3"(62·6 × 92·67m)
HAK	Schoharie Creek Headwaters	Hunter, Kaaterskill (NY)	564390m	4673430m	30m
HAKA2S	Schoharie Creek Headwaters	Hunter, Kaaterskill (NY)	564465m	4673415m	60m
SCHO	Schoharie Creek	Binghampton (NY)	74°17'06"	42°55'48"	3"(68·3 × 92·67m)
EDEL	East Deleware River	Binghampton (NY)	74°57'24"	42°04'30"	3"(68·3 × 92·67m)
RACOON	Racoon Creek	Hookstown, Midway, Burgettstown, Clinton, Alquippa, Avella (PA)	558270m	4495650m	30m
RACONDMA	Racoon Creek	Canton E (PA,OH,MN)	80°21'24"	40°39'27"	3"(70·5 × 92·67m)
BEAVER	Beaver Creek	Canton E (PA,OH,MN)	80°30'54"	40°38'42"	3"(70·5 × 92·67m)
BUCK	Buck Creek	Gasquet SW and SE, Ship Mtn. NW, NE, SW and SE, Dillon Mtn. NW and SW, Preston Peak SW (CA)	418350m	4620660m	30m
BRUSHY	Brushy Creek	Upshaw, Houston, Grayson, Massey, Moulton, Addison (AL)	433230m	4591290m	30m
MOSHANNON	Moshannon Creek	Ramey, Blandburg, Wallaceton, Houtzdale, Tipton, Philipsburg Sandy Ridge (PA)	735420m	4532580m	30m
TVA[1]	Montgomery Fork	Block (TE)	2492200[2]ft	707200[2]ft	100ft

Notes:
1. Obtained courtesy of the Tennessee Valley Authority, Maps and Surveys Department
2. Tennessee State plane coordinates in ft

of what support area to use is therefore important. Figure 2 shows networks extracted from a DEM with three different support areas (S_a) compared to the network inferred from contour crenulations and digitized from a topographic map. By specifying S_a the drainage density can be chosen arbitrarily for networks extracted from DEMs. In fact from dimensional analysis we expect the relationship

$$D_d \propto \frac{1}{\sqrt{S_a}} \tag{9}$$

This in fact holds approximately, with slightly different proportionality constants for each DEM.

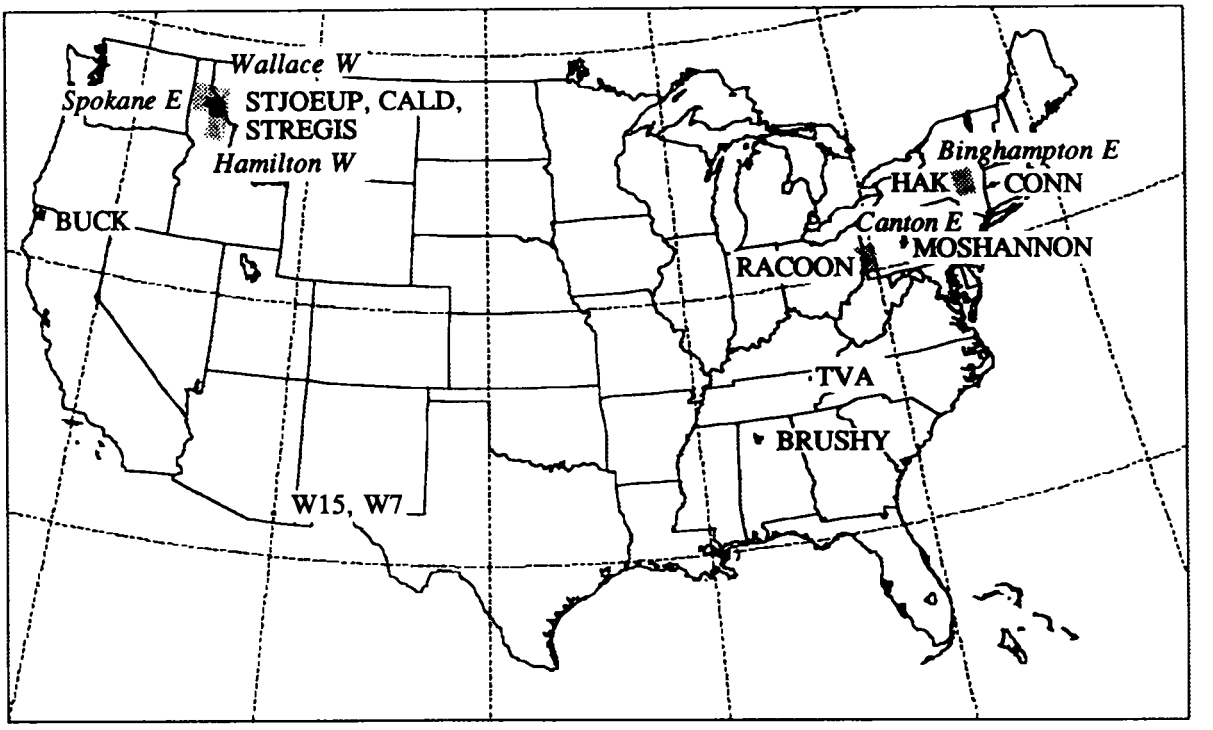

Figure 1. Location map. 7·5 min datasets are black, 1° DMA Quadrangles are shaded and labelled with italics

In extracting networks from DEMs we suggest that the networks extracted should have properties traditionally ascribed to channel networks and have as high resolution as possible. The procedures consist of looking for the smallest scale, measured in terms of support area, where the key elevation scaling laws (Constant drop property and power law scaling of slope with area) break. We argue elsewhere (Tarboton, 1989; Tarboton *et al.* in preparation) that this break point represents a physical transition from channel erosion and transport mechanisms at large scale to hillslope erosion and transport mechanisms at small scale. The hillslope transport processes are diffusive in nature whereas the channel mechanisms rely on the power of concentrated flow in channels.

Tarboton *et al.* (1988) showed that it was possible for the bifurcation and length laws to hold down to infinitely small scale in which case the channel network can be regarded as Fractal. The same can be said of the area law and any other empirical description of the planform structure of a river network. However, the

Table II. Statistics of adjustments required to fill pits

Data Set	Total Number of Pixels	Mean adjustment (m)	% of pixels adjusted	Number and percentage of pixels adjusted by amount 1-5 (m)	6-10 (m)	11-20 (m)	20+ (m)	Max (m)
CALD	600270	4·8	1·6	6656 (1·1%)	1839 (0·31%)	896 (0·15%)	136 (0·02%)	35
STREGIS	2009511	4·9	0·9	12382 (0·6%)	3424 (0·17%)	1768 (0·08%)	315 (0·02%)	44
MOSHANNON	1522962	2·6	4·7	64535 (4·2%)	5554 (0·4%)	786 (0·05%)	109 (0·007%)	89
Spokane E Quad.	1442401	11·2	3·7	20769 (1·4%)	6731 (0·47%)	6732 (0·47%)	19013 (1·3%)	61

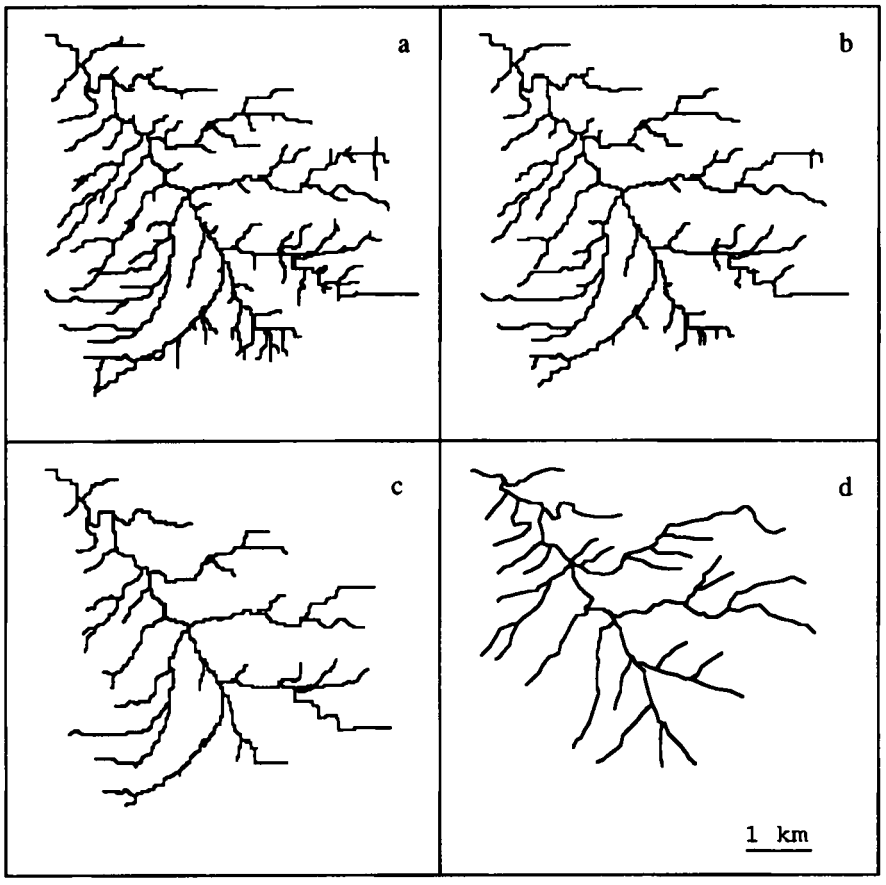

Figure 2. Channel Networks from DEM with varying support area compared to Blue Lines for the W15 dataset: (a) 50 pixels ($D_d = 3{\cdot}4\ km^{-1}$), (b) 100 pixels ($D_d = 2{\cdot}7\ km^{-1}$), (c) 200 pixels ($D_d = 2{\cdot}0\ km^{-1}$), (d) 'Blue Lines' ($D_d = 1{\cdot}7\ km^{-1}$)

power law scaling of slope with area represented as

$$S \propto A^{-\theta} \tag{10}$$

cannot hold over all ranges of scale in the landscape. In particular as A approaches zero, near the hilltops this would predict infinite slopes, a nonsensical result. The same can be said of the constant drop property and Hortons slope law in the limit of small order. After all, these are all elevation related scaling properties that describe the general concavity of channel profiles. We therefore suggest that a rational support area to use to extract channel networks is the smallest S_a for which these elevation related scaling properties still hold.

CONSTANT DROP PROCEDURES

Figure 3 shows the drops of all 142 streams in the magnitude 107, order 5 network extracted from the W15 data set with support area threshold of 50 (30 m × 30 m) pixels. Stream drops are highly variable and we need to test whether the constant drop property is valid in the sense that the mean drop is independent of stream order. The t statistic for the comparison of means of different populations (Beyer, 1984) is used to compare the mean drop for streams of different order.

$$t = \frac{\bar{x} - \bar{y}}{\sqrt{\dfrac{(n_x - 1)S_x^2 + (n_y - 1)S_y^2}{n_x + n_y - 2}}\sqrt{\dfrac{1}{n_x} + \dfrac{1}{n_y}}} \tag{11}$$

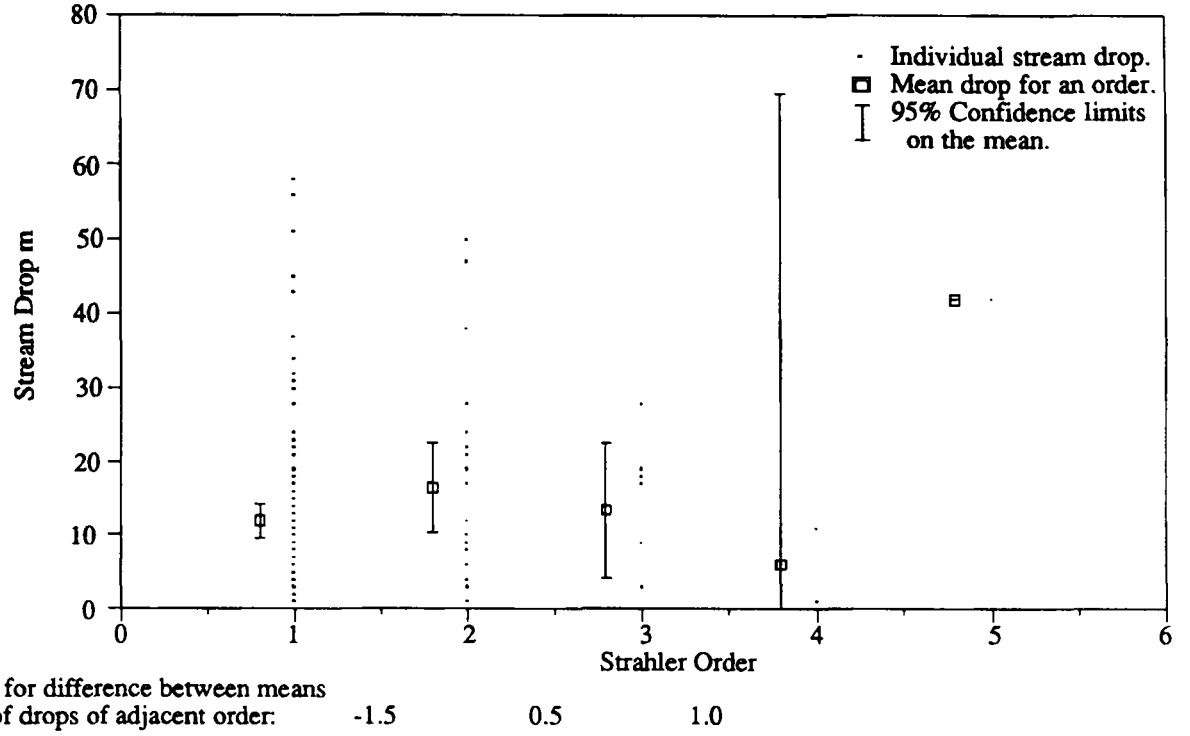

Figure 3. Stream drops in W15 network extracted using a support area of 50 pixels

where $\bar{x}$ and $\bar{y}$ are the sample means, S_x^2 and S_y^2 the sample variance, and n_x and n_y the sample sizes of the two populations x and y. The t for the difference between successive orders is given in Figure 3. That the t statistic has magnitude no larger than 2 indicates that the null hypothesis of no difference in the means cannot be rejected at the 95 per cent confidence level. This is also seen graphically in terms of 95 per cent confidence limits on the sample mean assuming it is t distributed. A horizontal line that passes through all the error bars could be drawn, indicating constant mean drop that is not significantly different from the sample mean drops at any order. In contrast, Figure 4 gives the case where a support area of 20 pixels has been used to define channel networks in the W15 catchment. Notice that the mean drop of first order streams is significantly less than the other mean drops. According to the t statistics, the break in scaling occurs between support areas of 20 and 50 pixels.

Dramatic evidence of the break in scaling is given by considering the stream drop probability distribution. This is done in Figure 5 for the W15 basin. Exceedance probabilities are calculated using the Weibull plotting position

$$P = \frac{i}{N+1} \tag{12}$$

where i is the ranking from smallest to largest and N is the number of streams in the sample; 95 per cent confidence limits computed from the beta distribution are shown. We see that the distribution of first order drops in the support area 20 network stands out from the other distributions which are all intermingled. This corroborates the difference between first order drops at support area 20, and other stream drops. Straight line fits on this semilog plot suggest the exponential distribution as a good model for stream drops, and that Strahler streams of different order have practically the same probability distribution above the point where scaling breaks. This is a probabilistic statement of the constant drop property.

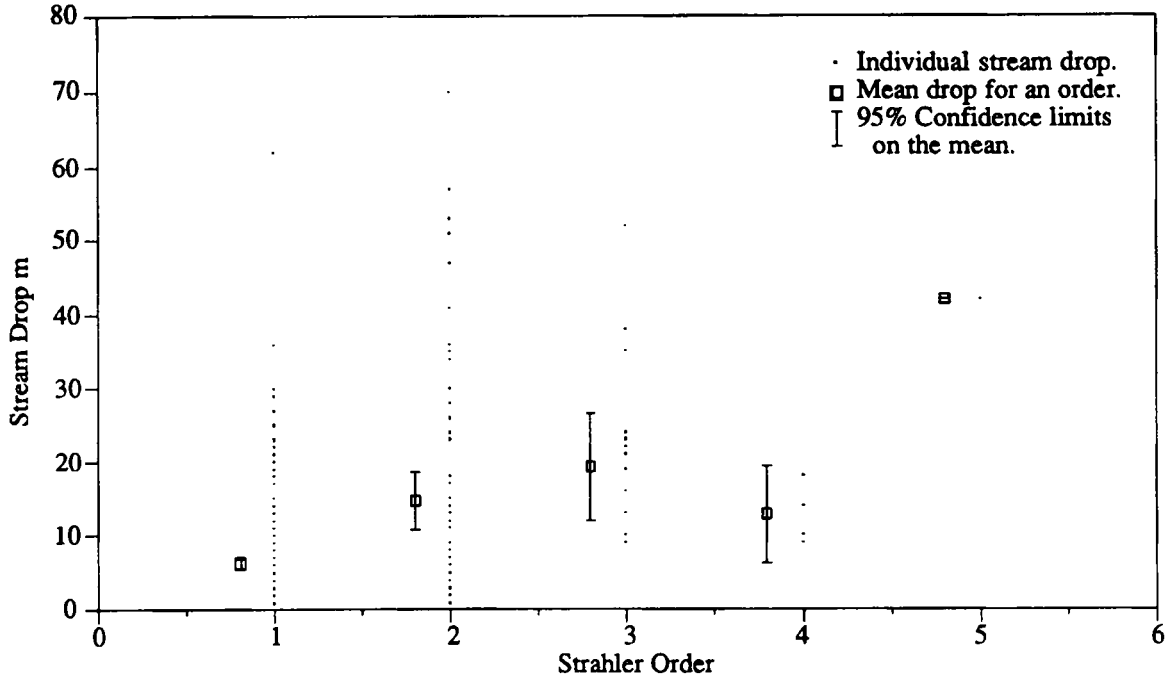

t for difference between means of drops of adjacent order: -6.7 -0.8 0.5

Figure 4. Stream drops in W15 network extracted using a support area of 20 pixels

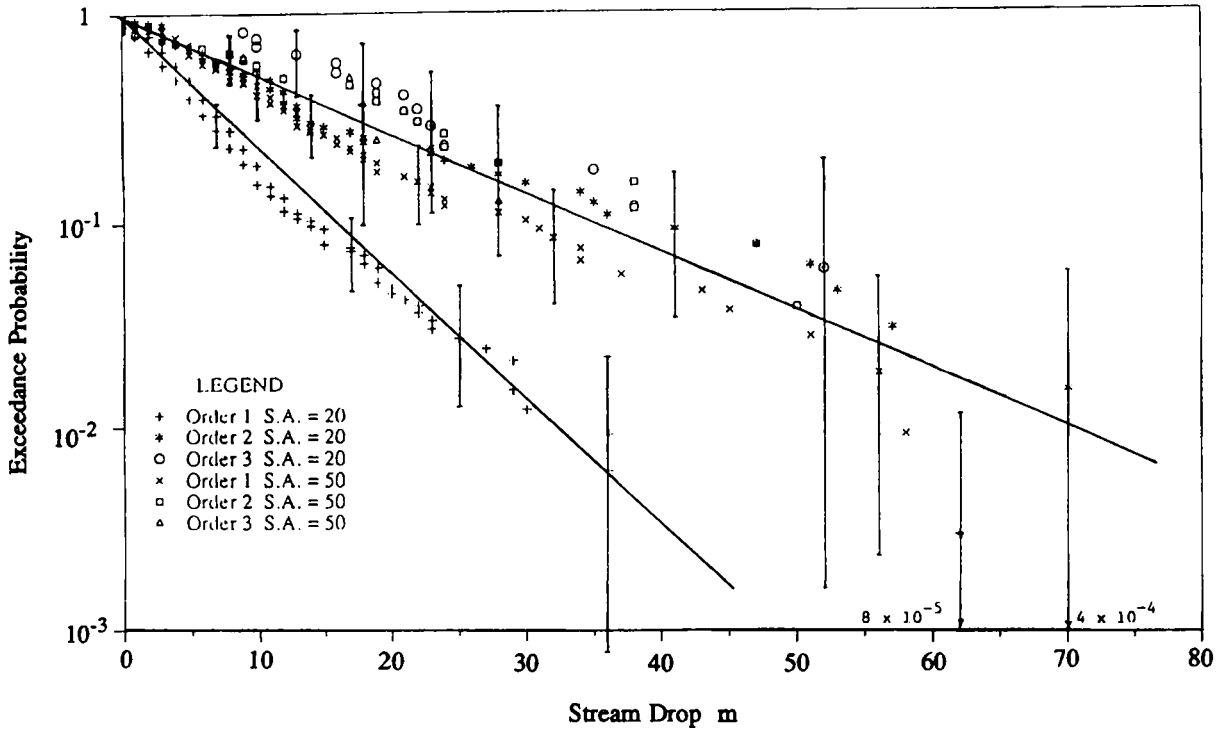

Figure 5. Stream drop distributions for the W15 network. S.A. in the legend denotes support area. Error bars are 95 per cent confidence limits using the Beta distribution

Tests for the break in scaling using the constant drop property can be done graphically with several plots like Figure 3 and 4 compressed into one plot. Figure 6 illustrates the results for the Big Creek basin. For each each support area the stream drops, mean drop, and 95 per cent confidence limits of the mean are plotted against order. Within each grouping order increases from left to right. Statistics, including the t statistic for the difference between mean first order stream drop and mean of all higher order stream drops are printed below the figure. To the left (small support area) of a limit or threshold support area, the constant drop property fails whereas to the right (large support area), the constant drop property holds. This limit, the smallest support area for which the constant drop property is not rejected, gives a measure of the basic horizontal length scale in the landscape, measured in terms of support area or drainage density. The drainage density obtained from this type of figure is listed in Table III for all the basins analysed, together with results from other procedures. A full set of figures similar to Figure 6 for all the basins analysed is given in Tarboton (1989).

The constant drop property is basically equivalent to $R_s = R_l$. Deviations from the constant drop property can be expected if $R_s \neq R_l$. Typical values for R_l and R_a are 2 and 4 respectively so Equation 8 gives $\theta = 0{\cdot}5$. The test for the break in the constant drop property is roughly equivalent a test for deviation from $\theta = 0{\cdot}5$. Different $R_s = R_l$ and R_a would result in a different scaling exponent θ here. The outcome of the constant drop analysis is basically two length scales. The horizontal length scale ($1/D_d$) and vertical length scale, mean stream drop H. The ratio of these HD_d gives a form of ruggedness number (see Strahler, 1964), which is a dimensionless number that characterizes the steepness of the channel network. We could speculate that it is related to climate, tectonic uplift, etc. Table III includes HD_d data for the basins we analysed.

SLOPE SCALING PROCEDURES

Figure 7 shows slope versus contributing area for links of a network where a small support area was used to extract the network. Area is total contributing area measured at the downstream end of each link and slope is mean link slope defined as the link height divided by link length. It is a link average slope at the scale the

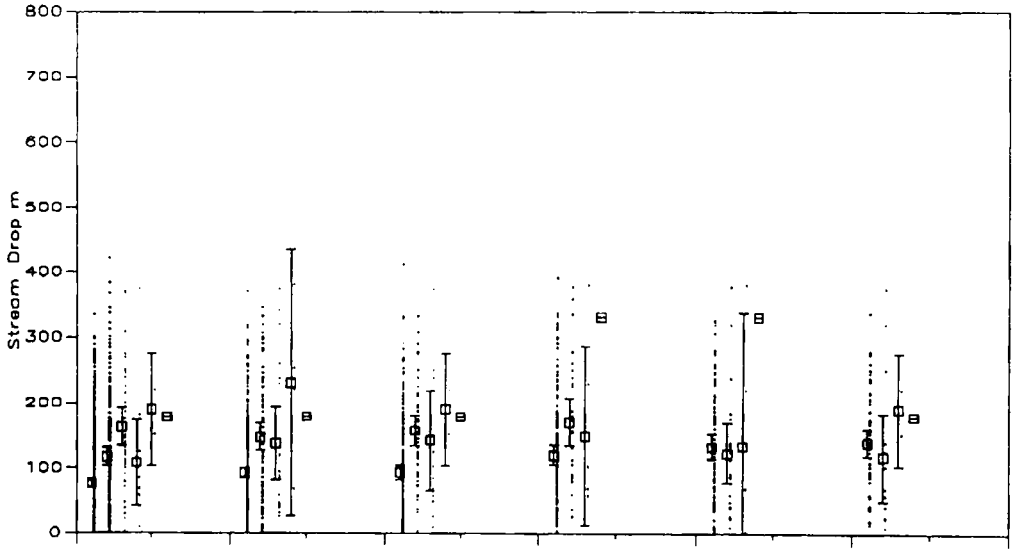

Support Area	50	100	200	300	500	800
Drainage Density (km^{-1})	2.7	1.9	1.4	1.2	0.94	0.78
Magnitude	846	400	223	139	87	57
t	9	6.7	5.4	2.8	0.02	0.3

Figure 6. Variation of stream drop with order and support area for the Big Creek (CALD) 7·5 min series dataset

Table III. Summary of landform scale results

Basin	Area (km^2)	Constant drop analysis A (km^2)	D_d (km^{-1})	H (m)	HD_d	Slope scaling analysis A_l (km^2)	A_b (km^2)	A_u (km^2)	D_d (km^{-1})	θ	Peuker Douglas D_d (km^{-1})
W7	12·8	0·09	2·5	18	0·045	0·0018[1]	0·0018[1]	0·0024	26·3	0·30	5·5
W15	22·7	0·045	3·4	15	0·051	0·0018[1]	0·0024	0·0045	19·4	0·29	4·7
W15A2S	22·7	0·072	2·7	15	0·039	*	*	*	*	0·25	3·3
CALD	146·9	0·27	1·2	130	0·16	0·16	0·19	0·24	1·3	0·51	3·19
SPOKBC	146·9	0·41	0·93	128	0·12	0·32	0·45	0·68	0·9	0·48	1·5
NELK	440·2	0·41	0·98	89	0·087	0·21	0·30	0·42	1·1	0·47	1·7
STJOE	2834	1·16	0·59	140	0·082	0·75	0·96	1·18	0·65	0·47	1·45
STJOEUP	384·6	0·27	1·1	114	0·13	0·30	0·34	0·40	1·0	0·56	3·03
STREGIS	786·6	0·63	0·81	148	0·12	0·45	0·53	0·61	0·88	0·55	3·01
STREGISDMA	796·2	0·89	0·71	139	0·098	0·98	1·52	2·65	0·56	0·55	1·45
HAK	98·2	0·18	1·6	48	0·077	0·044	0·076	0·12	2·76	0·48	5·19
HAKA2S	98·75	0·18	1·5	47	0·070	0·018	0·027	0·041	5·6	0·42	2·27
SCHO	2408	0·95	0·68	56	0·038	1·51	2·08	3·12	0·46	0·43	1·21
EDEL	933·0	1·9	0·47	73	0·034	0·98	1·43	2·07	0·51	0·55	1·24
RACOON	448·0	0·45	1·1	22	0·024	0·31	0·43	0·63	1·1	0·51	7·2
RACONDMA	480·1	0·65	0·86	16	0·014	*	*	*	*	0·34	2·14
BEAVER	1223	0·18	0·6	19	0·011	0·077	0·29	0·89	1·37	0·34	2·14
BUCK	606·2	0·9	0·69	191	0·013	0·32	0·37	0·41	1·1	0·48	4·47
BRUSHY	321·8	0·09	2·3	14·5	0·033	0·12	0·18	0·26	1·7	0·53	5·73
MOSHANNON	325·4	0·63	0·95	35·5	0·034	1·6	2·1	2·7	0·57	0·58	7·2
TVA	36·5	0·14	1·3	97·5	0·13	0·57	0·68	0·99	0·79	0·85	4·5

Key:
A Lowest Support Area for which constant drop property cannot be rejected
D_d Drainage density
H Mean stream drop
A_l Switch point lower 95% confidence bound
A_b Switch point with minimum residual sum of squares
A_u Switch point upper 95% confidence bound
θ Log(slope)-Log(area) scaling exponent above switch point

Notes:
1 At lower limit of range of possible switch points
* Could not be obtained or was not significant

network is extracted. Here the scale or support area of extraction of the network serves to define the length of averaging for computation of slopes. Figure 7 has significant scatter indicating that slope is highly variable. However, when many links with similar area are grouped together and averaged (circles in Figure 7) the mean slope is seen to follow a fairly smooth trend. The straight lines are fitted to the circles using two phase regression. The line to the right of the switch point, with negative slope, corresponds to the scaling described in Equation 7. The switch point gives the scale at which this scaling breaks and is the support area that we are suggesting should be used to extract channel networks from DEMs.

To objectively test for the break in scaling we use two-phase regression (Solow, 1987; Hinkley, 1969). The technique is applied to a set of ordered pairs (x_i, y_i), $i = 1, \ldots, n$, that are assumed to be related by

$$y_i = a_o + b_0 x_i + b(x_i - c)\mathrm{I}(x_i - c) + e_i \tag{13}$$

where a_0, b_o, b, and c are parameters in the regression. I(.) is the indicator function defined

$$\mathrm{I}(x) = \begin{cases} 0 & \text{for } x \leq 0 \\ 1 & \text{for } x > 0 \end{cases} \tag{14}$$

and e_i are the errors, assumed independently and identically distributed. The parameter c gives the switch point. The slope for $x < c$ is b and for $x > c$ is $b_o + b$. The parameters are estimated by minimizing the sum of

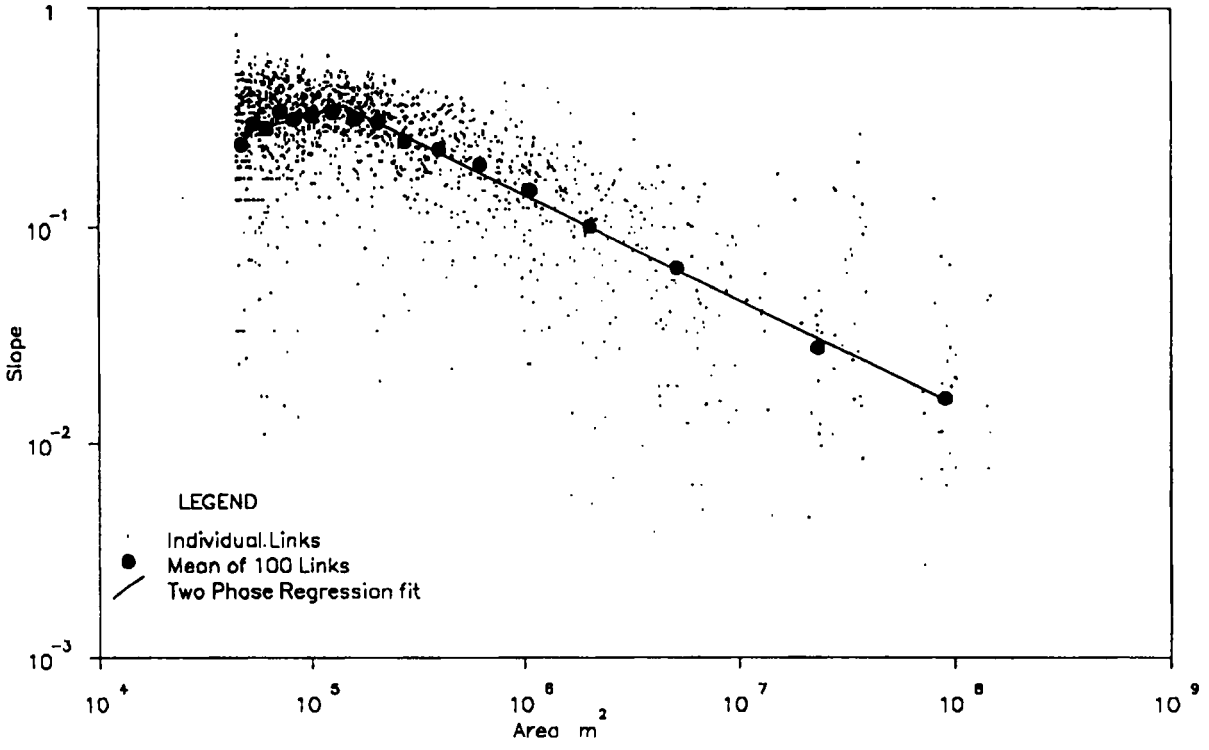

Figure 7. CALD (Big Creek, Idaho) Link slopes with support area of 50 pixels used to extract network

squares (SS) of the difference between y_i as observed and predicted by Equation 13. For c fixed SS is a quadratic function of a_o, b_o, and b which upon differentiation and equating to zero leads to the normal equations:

$$\begin{aligned} na_0 + \Sigma_1 x_i b_0 + (\Sigma_2 x_i - cn_2)b &= \Sigma_1 y_i \\ \Sigma_1 x_i a_o + \Sigma_1 x_i^2 b_o + (\Sigma_2 x_i^2 - c\Sigma_2 x_i)b &= \Sigma_1 x_i y_i \\ (\Sigma_2 x_i - cn_2)a_o + (\Sigma_2 x_i^2 - c\Sigma_2 x_i)b_o + (\Sigma_2 x_i^2 + c^2 n_2 - 2c\Sigma_2 x_i)b &= \Sigma_2 x_i y_i - c\Sigma_2 y_i \end{aligned} \tag{15}$$

where Σ_1 is the sum over all data (n), Σ_2 is the sum over points with $x_i > c$, and n_2 is the number of points with $x_i > c$. These can be solved to give values a_o, b_o, and b that minimize the sum of squares conditional on c. A grid search over possible values of c is then used to obtain the set a_o, b_o, b, c that minimizes SS. According to the model (13), these are maximum likelihood estimates of the parameters (Solow, 1987).

This regression should be tested against the null model, normal linear regression without a switch point.

$$y_i = a_n + b_n x_i \tag{16}$$

with residual sum of squares SS_o. Solow (1987) gives the likelihood ratio statistic

$$R = \frac{(SS_o - SS)/3}{SS/(n-4)} \tag{17}$$

The test is to reject the null hypothesis, that the two phase regression is not different from linear regression, at the $1 - \alpha$ level if

$$R \geq F_{3,n-4}(1 - \alpha) \tag{18}$$

where $F_{3,n-4}(1 - \alpha)$ is the $1 - \alpha$ quantile of the F distribution with 3 and $n - 4$ degrees of freedom.

Confidence intervals can be placed on the estimate of the switch point c. Following Solow (1987), the two-sided hypothesis that c is not significantly different from a reference value c' with significance level $1 - \alpha$ is accepted if

$$(SS' - SS)/[SS/(n - 4)] \leq F_{1,n-4}(1 - \alpha) \tag{19}$$

where SS' is the sum of squares from fitting model (13) conditional on $c = c'$. Then the $1 - \alpha$ confidence interval for c is the set of c' satisfying (19). For the data in Figure 7, the regression was done using the natural logs of the mean data (circles). Figure 8 shows the sum of squares, SS, versus c (switch point area) for this data. The minimum SS corresponding to a contributing area of 143×10^3 m^2 is clearly seen: 95 per cent confidence limits for the switch point are given by the portion of this graph below the threshold SS' determined from (19).

It is possible to apply this technique to slopes and areas of individual pixels, as well as slopes and areas of 'links' from a channel network with small support area. In principle the individual pixel data is like using a support area of 1 pixel to extract a network. The use of higher support areas just means slopes are averaged over longer distances thus reducing the effect of DEM data error. The following mean link lengths from the

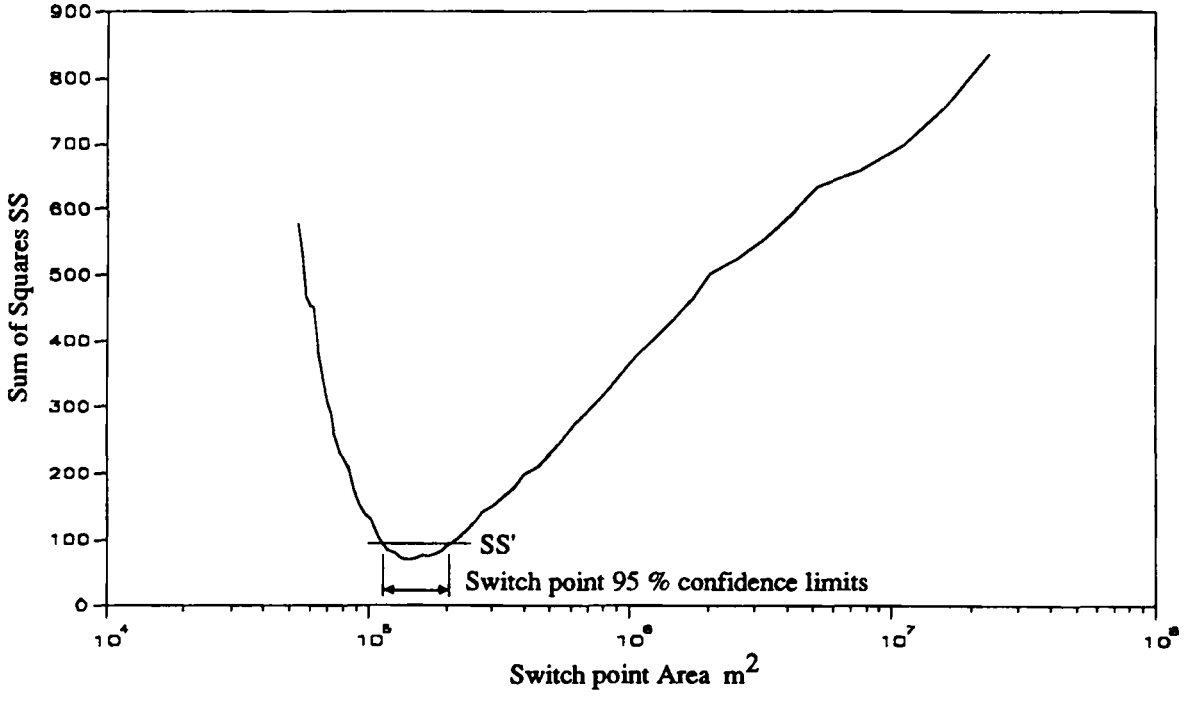

Figure 8. CALD (Big Creek, Idaho) Residual sum of squares from two phase regression as a function of switch point

W15 data set for different support areas give an idea of the averaging length associated with different support areas.

Support Area (No of Pixels)	1	5	10	20	50
Mean Link Length (m).	30	84	116	177	365

We have used both pixels and links as our unit of analysis. Figures 9(a) and 9(b) are typical results. In these the minimum number of points (pixels or links) averaged together was chosen large enough to minimize the scatter. This number is indicated in parentheses in the legend of each plot. Two phase regression was applied to all the points plotted. A full set of plots like these are given in Tarboton (1989). The drainage densities determined from using the break point in these figures as a support area to extract channel networks are given in Table III where they are compared to drainage density estimated from other techniques.

RESULTS

The above procedures have used a support area threshold to extract channel networks from DEMs. Scaling and breaks in that scaling were used to identify what we believe is the correct support area threshold. This section will compare the results to more direct procedures for identifying valleys within DEMs.

Band (1986) discusses the Peuker and Douglas (1975) algorithm for identifying concave pixels, to extract channel networks from DEMs. Figure 10 gives an example of pixels identified by such a procedure for the CALD data set. The main drainage paths are apparent, but the problem is that they are not connected, i.e. there are gaps. Band (1986) suggests procedures to connect these to form a network. These are not discussed here.

We should point out than in obtaining Figure 10 a moving average smoothing of the data was used. We used the simple smoothing kernel

0·05	0·1	0·05
0·1	0·4	0·1
0·05	0·1	0·05

Without smoothing the Peuker-Douglas algorithm performs poorly, identifying pixels that hardly resemble a network at all, presumably due to many adjacent pixels of the same elevation since elevations are given in integer metres.

The density of points in Figure 10 can be used to give an idea of the drainage density. A length (1/2 the length of a side + 1/2 the length of a diagonal) is associated with each channel pixel so drainage density is estimated from the number of identified pixels × length divided by area. For comparison with Figure 10, Figure 11 gives all pixels with accumulation area greater than 300 pixels for the CALD data set, which was the support area identified by the constant drop procedure.

Table III summarizes all the landform scale results, comparing drainage density estimated from the constant drop and break in scaling technique described previously and the Peuker-Douglas procedure. The drainage densities from the different techniques are also compared in Figure 12. The scatter about a straight line at 45° measures the degree of agreement between the different estimates of drainage density. Within the scatter there appears to be reasonable agreement between drainage densities obtained from slope scaling and

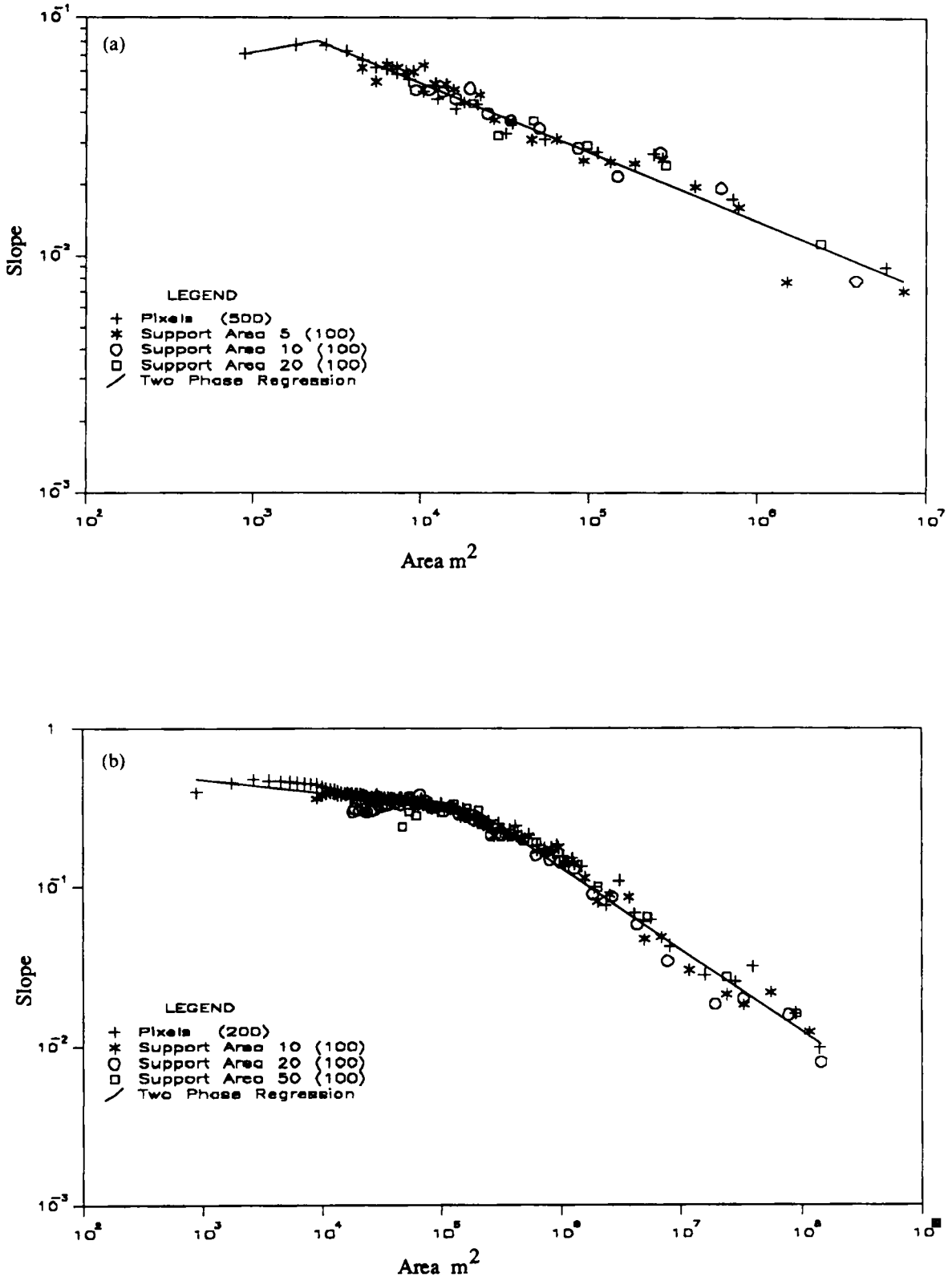

Figure 9. (a) W15 Slope versus Area and Two Phase Regression Plot; (b) CALD Slope versus Area and Two Phase Regression Plot

Figure 10. Pixels identified by the Peuker and Douglas Algorithm applied to the CALD dataset

the constant drop analysis. The agreement with the Peuker-Douglas D_d is not as good and there appears to be a bias with the Peuker-Douglas procedure consistently over estimating drainage density relative to the other two procedures. Perhaps this is due to the Peuker-Douglas procedure being more sensitive to local differences and errors in the data or an error in the length associated with each pixel.

DISCUSSION

Evaluation of these results raises the following concerns: Are the scales (drainage density) obtained dependent on data resolution and data set size? What is the effect of data errors? To address the first concern, five pairs of data sets are actually the same river basin with DEMs of different pixel size. These are (W15, W15A2S), (HAK, HAKA2S), (CALD, SPOKBC), (STREGIS, STREGISDMA), and (RACOON, RACOONDMA). In the first two of these the low resolution DEM was formed from the high resolution DEM by averaging together the elevations of four adjacent pixels. In the other three the low resolution data set is a

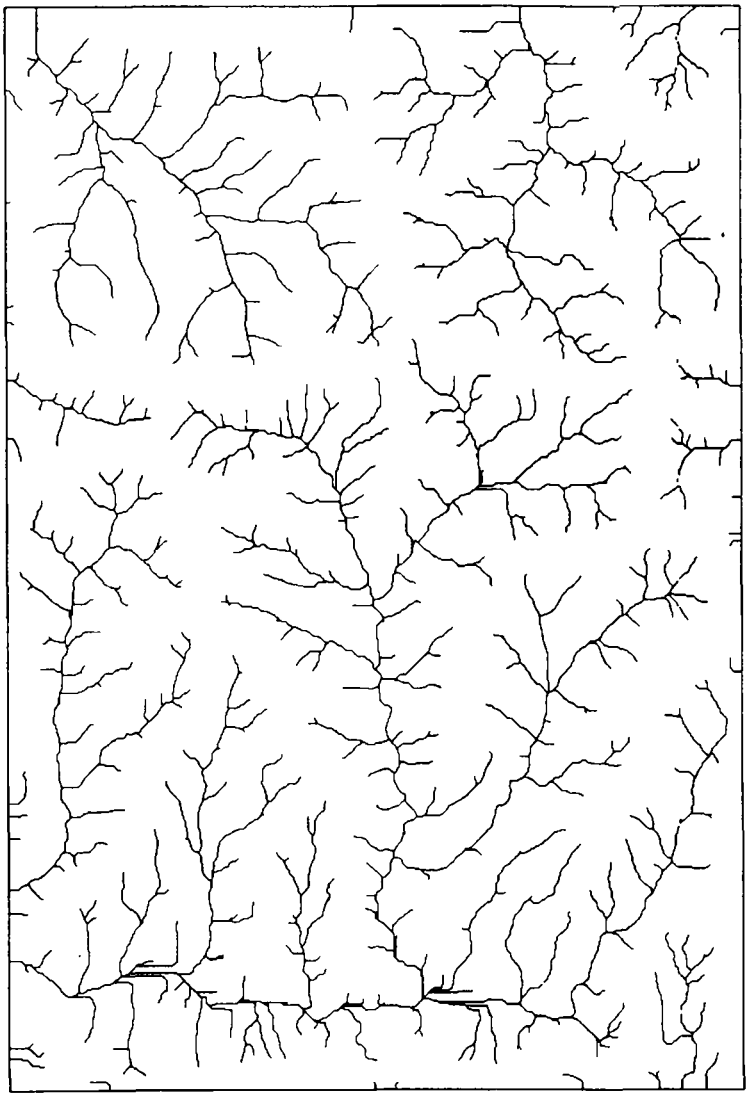

Figure 11. Pixels that exceed accumulation area threshold of 300 pixels in the CALD dataset

defense mapping agency data set on three arc second grid while the high resolution data set is a U.S.G.S. data set on 30 m grid. We see that the drainage densities obtained from the constant drop analysis agree fairly well for all five of these data sets. The comparison of slope scaling drainage densities for the (CALD, SPOKBC) and (STREGIS, STREGISDMA) pairs is also good. For the (HAK, HAKA2S) pair the slope scaling drainage density comparison is not good and also differs from the constant drop drainage density. For the RACOONDMA and W15A2S data sets the slope scaling does not give a detectable break so the comparison cannot be made.

Some of the data sets are also nested. CALD and STJOEUP are subbasins within STJOE and HAK is a subbasin within SCHO. Analysis of these suggests a higher drainage density for the subbasin, possibly some indication of a data set size or scale effect. In principle if the drainage density was uniform, D_d of the subbasins should be the same as the D_d of the larger enclosing basin. This is not the case. STJOE has $D_d \approx 0{\cdot}5\ \text{km}^{-1}$ while CALD and STJOEUP have $D_d \approx 1\ \text{km}^{-1}$. SCHO has $D_d \approx 0{\cdot}7\ \text{km}^{-1}$ while the subbasin HAK has $D_d \approx 1{\cdot}7\ \text{km}^{-1}$. The subbasins are from higher resolution data, but the comparisons in the previous paragraphs suggest this should not have an effect.

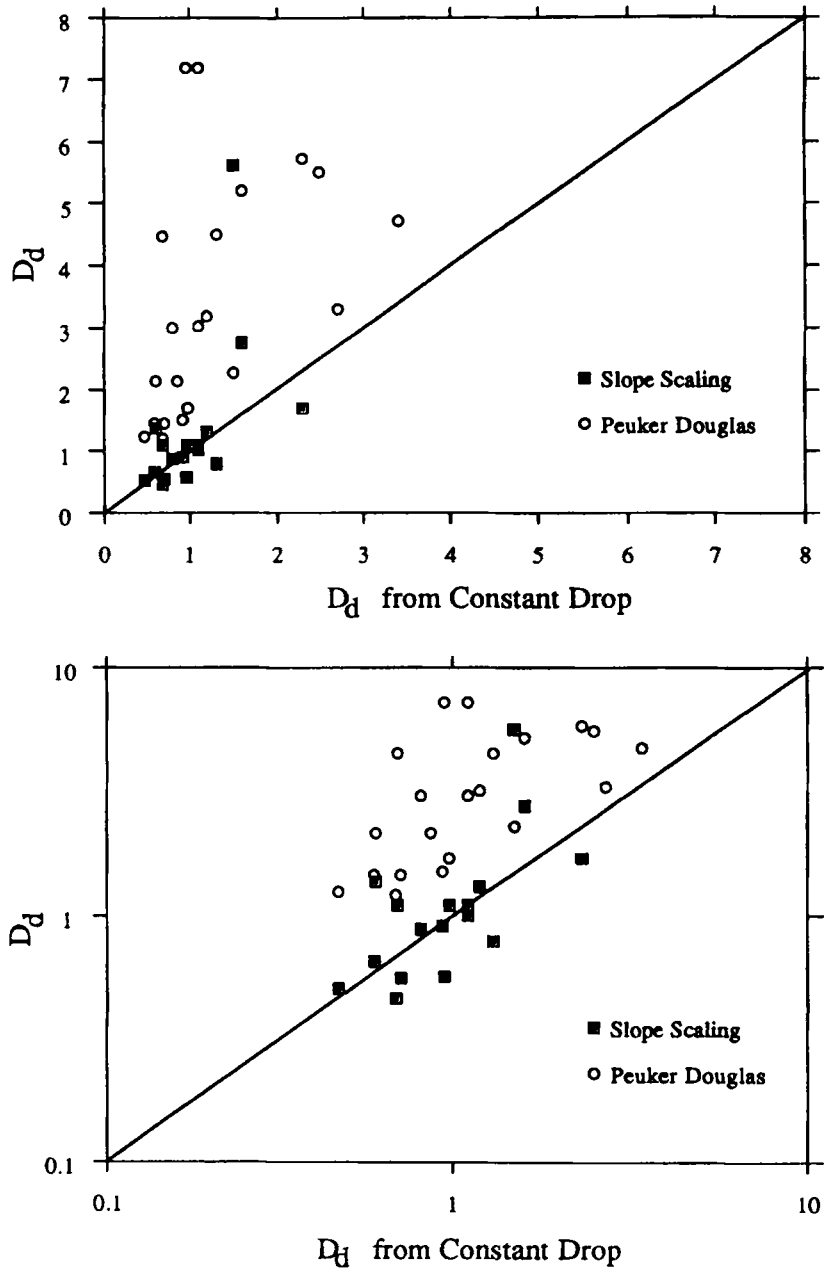

Figure 12. Comparison of drainage density from different techniques

A possible explanation is that larger basins imply more streams and a larger sample size for detection of trends or breaks in scaling, so for larger basins our scale detection threshold may be lower, an undesirable basin size effect in the results. Another explanation is that drainage density may be variable within the basins, due to variation of geologic or climatic factors. The large basins (SCHO and STJOE) have lengths of the order of 50-100 km, in which it is entirely plausible that D_d could vary considerably. The scale at which a break occurs then becomes a range of scales, corresponding to a range of drainage densities within the data set. If there is a lot of data statistical rejection of constant drops or slope scaling may occur at the low drainage density end of the range of drainage densities present. This range is expected to be wider for larger

data sets, hence the scale effect. It is not possible with the information at hand to resolve this issue and further research on this point may be warranted.

Random errors and the fact that DEM data is reported in integer metres has a large effect on the estimation of local slope, perhaps one reason for the scatter in Figure 7. At the scale of a single (30 m) pixel the integer data does not allow us to resolve slopes between $1/30 = 0{\cdot}033$ and 0. We attempt to avoid this effect by averaging over larger lengths using higher support areas. This had the effect of smoothing slope estimates at the expense of some resolution of areas. Areas smaller than the support area threshold used cannot be resolved. This results in a scale effect, apparent in Figure 9(b), where the break in slope is much more marked for the higher support areas and also appears to occur at a higher area for higher support areas. The two phase regression on all the data is a form of compromise between wanting accurate slope estimates and good area resolution.

Tarboton (1989) provides an analysis of the effect of random errors and shows that they can result in a bias in the gradient measured in slope area plots. This is most marked for single pixels where there is no benefit of averaging. To understand this effect consider an error in the elevation of a single pixel. If the error reduces the apparent elevation of a pixel, the apparent slope is reduced. This is because the slope of a pixel is measured as the difference in elevation between the pixel in consideration and its downslope neighbour, divided by the distance between pixels. Also adjacent pixels are more likely to drain towards the pixel in consideration due to its reduced elevation, thus increasing the apparent area that it drains. Similarly, an error that increases the apparent elevation increases slope and reduces area so the net effect is that errors result in a negative correlation between slope and area or negative slope in slope-area plots.

Despite the effect of errors we are able to detect fundamental or basic scales where the constant drop and slope-area scalings break. Since practically all channel networks have these properties it is sensible that they should be present in networks extracted from DEMs. This places a limit on how finely the network should be resolved and suggests a support area that should be used to extract channel networks from DEMs. The agreement between constant drop analysis and slope-area scaling shows that they are consistent and therefore complementary techniques for estimating drainage density. The drainage density obtained from these techniques corresponds fairly well to drainage density estimated from the altogether different local Peuker and Douglas (1975) procedures for detecting upward concave pixels in DEMs. The procedures proposed have justification in terms of network properties and are therefore preferable to procedures based on local curvature. Of the two procedures proposed, the analysis of stream drops seemed more robust than the analysis of slope scaling which was more susceptible to data errors.

ACKNOWLEDGEMENTS

Support for this work was provided by the National Science Foundation (Grant No. ECE-8513556) and through a cooperative agreement between the University of Florence and MIT.

REFERENCES

Band, L. E. 1986. 'Topographic partition of watersheds with digital elevation models', *Water Resources Research*, **22**(1), 15-24.

Beyer, W. H. 1984. *CRC Standard Mathematical tables*, CRC Press, Inc, Boca Raton, Florida.

Broscoe, A. J. 1959. 'Quantitative analysis of longitudinal stream profiles of small watersheds', *Office of Naval Research, Project NR 389-042*, Technical Report No. 18, Department of Geology, Columbia University, New York.

Carrara, A. 1988. 'Drainage and divide networks derived from high fidelity digital terrain models', In Chung, C. F. *et al.* (Eds), *Quantitative Analysis of Mineral and Energy Resources*, NATO ASI Series C, Mathematical and Physical Sciences, Vol. 223, Proceedings of the NATO Advanced Study Institute, Italy, June 22-July 4, 1986, D. Reidel Publishing Company.

Flint, J. J. 1974. 'Stream gradient as a function of order, magnitude and discharge', *Water Resources Research*, **10**(5), 969-973.

Gupta, V. K. and Waymire, E. 1989. 'Statistical self-similarity in river networks parameterized by elevation', *Water Resources Research*, **25**(3), 463-476.

Hinkley, D. V. 1969. 'Inference about the intersection in two phase regression', *Biometrica*, **56**(3), 495-504.

Horton, R. E. 1932. 'Drainage basin characteristics', *Transactions American Geophysical Union*, **13**, 350-361.

Horton, R. E. 1945. 'Erosional development of streams and their drainage basins: hydrophysical approach to quantitative morphology', *Geological Society of America Bulletin*, **56**, 275-370.

Jenson, S. K. and Domingue, J. O. 1988. 'Extracting Topographic Structure from Digital Elevation Data for Geographic Information System Analysis', *Photogrammetric Engineering and Remote Sensing*, **54**(11), 1593-1600.

Leopold, L. B. and Maddock, T. 1953. 'The hydraulic geometry of stream channels and some physiographic implications', *U.S. Geol. Surv. Prof. Paper*, **252**.

Leopold, L. B. and Miller, J. P. 1956. 'Ephemeral streams—hydraulic factors and their relation to the drainage net', *U.S. Geol. Survey Prof. Paper*, **282-A**.

Leopold, L. B., Wolman, M. G., and Miller, J. P. 1964. *Fluvial Processes in Geomorphology*, W. H. Freeman, San Francisco.

Mark, D. M. 1988. 'Network models in geomorphology', *Modelling in Geomorphological Systems*, John Wiley.

Moore, I., O'Loughlin, E. M., and Burch, G. J. 1988. 'A contour based topographic model for hydrological and ecological applications', *Earth Surface Processes and Landforms*, **13**, 305-320.

O'Callaghan, J. F. and Mark, D. M. 1984. 'The extraction of drainage networks from digital elevation data', *Computer Vision, Graphics and Image Processing*, **28**, 328-344.

O'Loughlin, E. M. 1986. 'Prediction of surface saturation zones in natural catchments by topographic analysis', *Water Resources Research*, **22**(5), 794-804.

Palacios-Velez, O. L. and Cuevas-Renaud, B. 1986. 'Automated river-course, ridge and basin delineation from digital elevation data', *Journal of Hydrology*, **86**, 299-314.

Peuker, T. K. and Douglas, D. H. 1975. 'Detection of surface-specific points by local parallel processing of discrete terrain elevation data', *Computer Graphics and Image Processing*, **4**, 375-387.

Schumm, S. A. 1956. 'Evolution of drainage systems and slopes in Badlands at Perth Amboy, New Jersey', *Geological Society of America Bulletin*, **67**, 597-646.

Shreve, R. L. 1966. 'Statistical law of stream numbers", *Journal of Geology*, **74**, 17-37.

Solow, A. R. 1987. 'Testing for climate change: an application of the two phase regression model', *Journal of Climate and Applied Meteorology*, **26**, 1401-1405.

Strahler, A. N. 1952. 'Hypsometric (area altitude) analysis of erosional topography', *Geological Society of America Bulletin*, **63**, 1117-1142.

Strahler, A. N. 1957. 'Quantitative analysis of watershed geomorphology', *Transactions American Geophysical Union*, **38**, 913-920.

Strahler, A. N. 1964. 'Quantitative geomorphology of drainage basins and channel networks', *Handbook of applied hydrology*, McGraw-Hill Book Co., New York.

Tarboton, D. G. 1989. *The analysis of river basins and channel networks using digital terrain data*, Sc.D. Thesis, Department of Civil Engineering, M.I.T. (Also available as Tarboton D. G., Bras, R. L., and Rodriguez-Iturbe, I. (Same title), Technical report no 326, Ralph M. Parsons Laboratory for Water resources and Hydrodynamics, Department of Civil Engineering, M.I.T., September 1989).

Tarboton, D. G., Bras, R. L., and Rodriguez-Iturbe, I. 1988. 'The fractal nature of river networks', *Water Resources Research*, **24**(8), 1317-1322.

Tarboton, D. G., Bras, R. L., and Rodriguez-Iturbe, I. 1989. 'Scaling and elevation in river networks', *Water Resources Research*, **25**(9), 2037-2051.

Wolman, M. G. 1955. 'The natural channel of Brandywine Creek, Pennsylvania', *U.S. Geological Survey Prof. Paper*, **272**, 56.

Yang, C. T. 1971. 'Potential energy and stream morphology', *Water Resources Research*, **7**(2), 311-322.